NAVAL POSTGRADUATE SCHOOL

MONTEREY, CALIFORNIA

THESIS

EFFECT OF PYROLYSIS PARAMETERS ON SILICON CARBIDE-FORMING COMPOSITE MIXTURES

by

James P. Agan

June 2021

Thesis Advisor: Ibrahim E. Gunduz
Second Reader: Troy Ansell

THIS PAGE INTENTIONALLY LEFT BLANK

REPORT DOCUMENTATION PAGE			*Form Approved OMB No. 0704-0188*

1. AGENCY USE ONLY *(Leave blank)*	**2. REPORT DATE** June 2021	**3. REPORT TYPE AND DATES COVERED** Master's thesis

4. TITLE AND SUBTITLE EFFECT OF PYROLYSIS PARAMETERS ON SILICON CARBIDE-FORMING COMPOSITE MIXTURES	**5. FUNDING NUMBERS**
6. AUTHOR(S) James P. Agan	
7. PERFORMING ORGANIZATION NAME(S) AND ADDRESS(ES) Naval Postgraduate School Monterey, CA 93943-5000	**8. PERFORMING ORGANIZATION REPORT NUMBER**
9. SPONSORING / MONITORING AGENCY NAME(S) AND ADDRESS(ES) N/A	**10. SPONSORING / MONITORING AGENCY REPORT NUMBER**

11. SUPPLEMENTARY NOTES The views expressed in this thesis are those of the author and do not reflect the official policy or position of the Department of Defense or the U.S. Government.

12a. DISTRIBUTION / AVAILABILITY STATEMENT Approved for public release. Distribution is unlimited.	**12b. DISTRIBUTION CODE** A

13. ABSTRACT (maximum 200 words)

High-performance ceramics are often used for reusable spacecraft Thermal Protection Systems (TPS). Pre-ceramic polymers provide a suitable route for fabricating silicon carbide (SiC)–based TPS. It is known that different phases of SiC form upon pyrolysis depending on the temperature. This research investigates the effects of pyrolysis temperature and nucleation aids on SiC forming pre-ceramic polymers and how they influence the final phases. It is possible that the addition of seed powders consisting of microscale and nanoscale SiC powders can aid growth of crystalline SiC at lower temperatures and influence the final composition in mixtures of SiC-forming polymers with crystalline SiC powders and graphite. For this research, pre-ceramic polymer mixtures with various nucleation aids were cured slowly in a furnace and pyrolyzed at various temperatures into a ceramic. The effects of temperature were investigated for six different sample configurations: pure polymer sample, micron crystalline SiC powder layer with polymer fill, nano SiC powder with polymer fill, micron SiC powder and polymer mixture (85 wt%), 3D printed amorphous carbon-loaded polylactic acid layer with SiC polymer fill, and crystalline graphite mixed with a UV-curable polymer (65 wt.%) mixed with SiC polymer. Material characterization was conducted via SEM to identify the phases. These results can improve processing procedures for these ceramics with better strength and thermal diffusivity for TPS.

14. SUBJECT TERMS additive manufacturing , polymer-derived ceramics, polymer infiltration, pyrolysis, silicon carbide, X-ray powder diffraction, energy-dispersive X-ray spectroscopy, pre-ceramic polymers, scanning electron microscopy, thermal protection system	**15. NUMBER OF PAGES** 59
	16. PRICE CODE

17. SECURITY CLASSIFICATION OF REPORT	**18. SECURITY CLASSIFICATION OF THIS PAGE**	**19. SECURITY CLASSIFICATION OF ABSTRACT**	**20. LIMITATION OF ABSTRACT**
Unclassified	Unclassified	Unclassified	UU

NSN 7540-01-280-5500

Standard Form 298 (Rev. 2-89)
Prescribed by ANSI Std. 239-18

THIS PAGE INTENTIONALLY LEFT BLANK

Approved for public release. Distribution is unlimited.

EFFECT OF PYROLYSIS PARAMETERS ON SILICON CARBIDE-FORMING COMPOSITE MIXTURES

James P. Agan
Ensign, United States Navy
BS, United States Naval Academy, 2020

Submitted in partial fulfillment of the
requirements for the degree of

MASTER OF SCIENCE IN MECHANICAL ENGINEERING

from the

NAVAL POSTGRADUATE SCHOOL
June 2021

Approved by: Ibrahim E. Gunduz
Advisor

Troy Ansell
Second Reader

Garth V. Hobson
Chair, Department of Mechanical and Aerospace Engineering

THIS PAGE INTENTIONALLY LEFT BLANK

ABSTRACT

High-performance ceramics are often used for reusable spacecraft Thermal Protection Systems (TPS). Pre-ceramic polymers provide a suitable route for fabricating silicon carbide (SiC)–based TPS. It is known that different phases of SiC form upon pyrolysis depending on the temperature. This research investigates the effects of pyrolysis temperature and nucleation aids on SiC forming pre-ceramic polymers and how they influence the final phases. It is possible that the addition of seed powders consisting of microscale and nanoscale SiC powders can aid growth of crystalline SiC at lower temperatures and influence the final composition in mixtures of SiC-forming polymers with crystalline SiC powders and graphite. For this research, pre-ceramic polymer mixtures with various nucleation aids were cured slowly in a furnace and pyrolyzed at various temperatures into a ceramic. The effects of temperature were investigated for six different sample configurations: pure polymer sample, micron crystalline SiC powder layer with polymer fill, nano SiC powder with polymer fill, micron SiC powder and polymer mixture (85 wt%), 3D printed amorphous carbon-loaded polylactic acid layer with SiC polymer fill, and crystalline graphite mixed with a UV-curable polymer (65 wt.%) mixed with SiC polymer. Material characterization was conducted via SEM to identify the phases. These results can improve processing procedures for these ceramics with better strength and thermal diffusivity for TPS.

THIS PAGE INTENTIONALLY LEFT BLANK

TABLE OF CONTENTS

THIS PAGE INTENTIONALLY LEFT BLANK

LIST OF FIGURES

LIST OF TABLES

THIS PAGE INTENTIONALLY LEFT BLANK

LIST OF ACRONYMS AND ABBREVIATIONS

AM	Additive Manufacturing
ASTM	American Society for Testing and Materials
BJ	Binder Jetting
C-SiC	Carbon-Silicon Carbon
CMC	Ceramic Matrix Composite
CT	X-Ray Computed Tomography
CVI	Chemical Vapor Infiltration
$^{\circ}$C	Degrees Celsius (SI Unit for Temperature)
DED	Directed Energy Deposition
EDS	Energy Dispersive X-Ray Spectroscopy
LSI	Liquid Silicon Infiltration
ME	Material Extrusion
MJ	Material Jetting
MSL	Mars Science Lab
NASA	National Aeronautics and Space Administration
PBF	Powder Bed Fusion
PCP	Pre-Ceramic Polymer
PCS	Polycarbosilanes
PICA	Phenolic Impregnated Carbon Ablator
PIP	Polymer Infiltration and Pyrolysis
PLA	Polylactic Acid
RCG	Reaction Cured Glass
SEM	Scanning Electron Microscope
SiC	Silicon Carbide
SL	Sheet Lamination
SLA	Stereolithography
SMP	Silicon Carbide Matrix Precursor
SPD	Space Policy Directive
TEM	Transmission Electron Microscopy
TPS	Thermal Protection System

TUFI	Toughened Unipiece Fibrous Insulation
TUFROC	Toughened Unipiece Fibrous Reusable Oxidation Resistant Ceramic
TVAC	Thermal Vacuum Oven
UV	Ultraviolet
VAP	Vibration Assisted Printing
VP	Vat Polymerization
wt.	weight
XRD	X-Ray Powder Diffraction

ACKNOWLEDGMENTS

I would like to thank my advisor, Dr. Emre Gunduz. This research would not have been possible without his guidance and support. From technical knowledge to hands-on laboratory training, his assistance was immensely appreciated from the beginning to the end.

I would also like to thank Dr. Troy Ansell for his training with material characterization equipment and his volunteering to serve as my second reader. He dedicated several hours to aid in my research. My gratitude for his patience and time cannot be overstated.

THIS PAGE INTENTIONALLY LEFT BLANK

I. INTRODUCTION

A. MOTIVATION

The space domain is an ever-expanding field of study with potential to benefit scientific, commercial, and military communities for various applications. One example of the benefits the space domain has to offer is satellites; they have several capabilities including, but not limited to, the gathering of information for meteorological purposes, imaging planets and other aspects of space, and communications across the globe. Many satellites and space probes are designed to be launched into space with no plan for reentry into Earth's atmosphere including an intact landing on the surface. This is not the case for manned space missions, which require the safe return of those on board and any intelligence collected.

Space Policy Directives (SPDs) outline space policy for the United States. SPDs call directly for more space missions beyond low Earth orbit; this specifically includes missions to the Moon, Mars, and other celestial bodies [1]. There is also a push for U.S. leadership in the commercial use of space as well as the growth of the U.S. Space Force [1]. Because of this, there is a need for the development of effective and reliable materials for space missions.

To ensure the safe return of spacecraft to Earth, a Thermal Protection System (TPS), commonly called heat shielding is used. Throughout the history of space exploration, several concepts and materials have been studied and used for TPS and implemented in the Apollo and Space Shuttle programs.

TPS materials are characterized as either ablative or non-ablative. Ablative materials deteriorate sacrificially under extreme conditions to protect what is underneath. Material is removed via the "combination of thermo-mechanical, thermo-chemical, and thermo-physical factors with a high temperature, pressure, and velocity of combustion flame" [2]. An example of an ablative material used for TPS is Avcoat, which was used during the Apollo missions (Figure 1) [3]. The material was effective; however, it was a single-use material that required assembly by hand to manufacture [3]. Ablative TPS

materials only offer a single use and are therefore not cost effective. Non-ablative materials, which are reusable, are required for a spacecraft to survive multiple launches and safe returns to Earth.

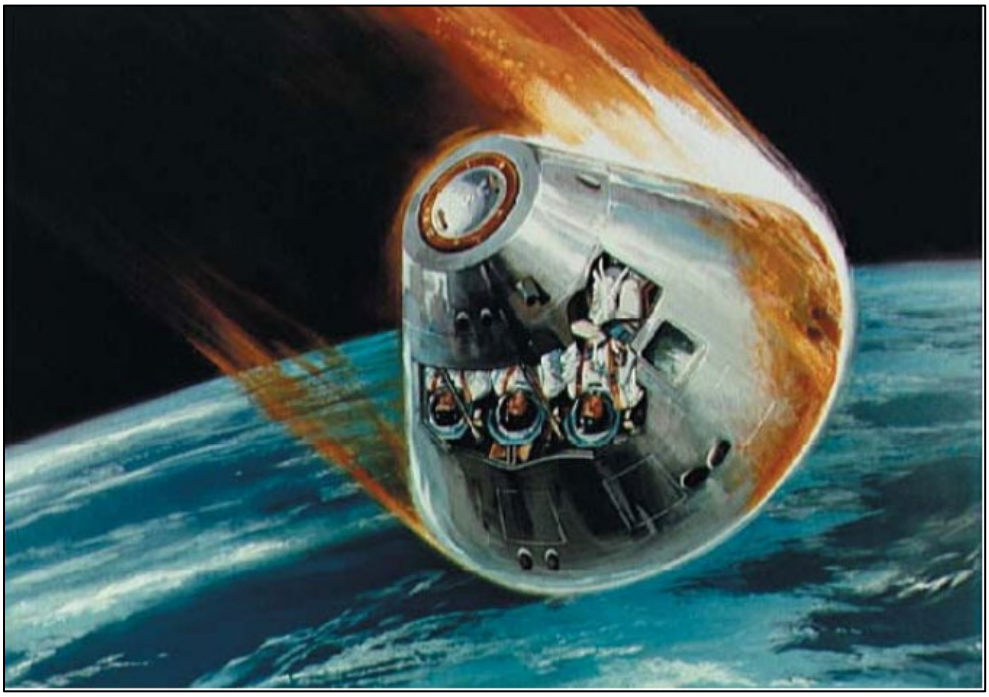

Figure 1. Artistic Concept of Apollo Capsule Re-entry. Source: [4].

While cost-effectiveness is desirable, it is required to maintain a significant level of protection and reliability to offer feasible substitutes as TPS materials. They must retain their mechanical and thermal properties without deterioration even under the extreme conditions associated with atmosphere re-entry. An example of a non-ablative material used for TPS is silica-based tiles used during over 100 shuttle missions [3]. Due to sustained damage to the tiles, Reaction Cured Glass (RCG) and Toughened Unipiece Fibrous Insulation (TUFI) coatings have been implemented to provide further protection to the spacecraft to improve durability [3]. Additionally, a two-piece approach has been developed called the Toughened Unipiece Fibrous Reusable Oxidation Resistant Ceramic (TUFROC) [3]. The development of materials for even more effective TPS continues.

Ideally, a TPS is re-usable. This requires a non-ablative material that is strong, lightweight, capable of surviving extreme environments, and simple and inexpensive to manufacture. The ability to easily repair or replace components is also desirable. Low thermal conductivity normal to the surface and high in-plane thermal conductivity is necessary to redistribute heat without damaging the substructure. This research explores specific methods of manual additive manufacturing to produce post-polymer ceramic composites designed to exhibit properties suitable for TPS materials.

B. BACKGROUND

1. History of TPS Materials

U.S. space exploration began in the 1960s. Its first satellite, Explorer 1, entered Earth's orbit in 1958, Alan Shepard became the first American in space in 1961, and John Glenn became the first American to orbit the Earth in 1962 [5]. President John F. Kennedy set a goal to send a man to the moon and get him back safely within the next decade in 1961; that goal was achieved in 1969 when Neil Armstrong, Buzz Aldrin, and Michael Collins completed this mission [5]. Since then, the United States has continued to send men and women into space as well as numerous satellites. Project Mercury and Project Gemini were the United States' first and second human spaceflight programs, respectively. They required TPS to withstand a re-entry velocity of 7.9 km/s; the Apollo program required capsules to withstand a re-entry velocity of 11 km/s, generating an aerodynamic heating environment nearly four times as extreme as capsules from the earlier programs [6]. The space domain continues to grow and requires effective and reliable material for TPS to guarantee a safe return.

As mentioned earlier, Avcoat was selected as the TPS material for the Apollo capsule. It served as the outer layer that would sacrificially deteriorate to protect the rest of the system. The TPS system also consisted of several other layer consisting of insulation as well as metallic honeycomb structures (Figure 2) [6].

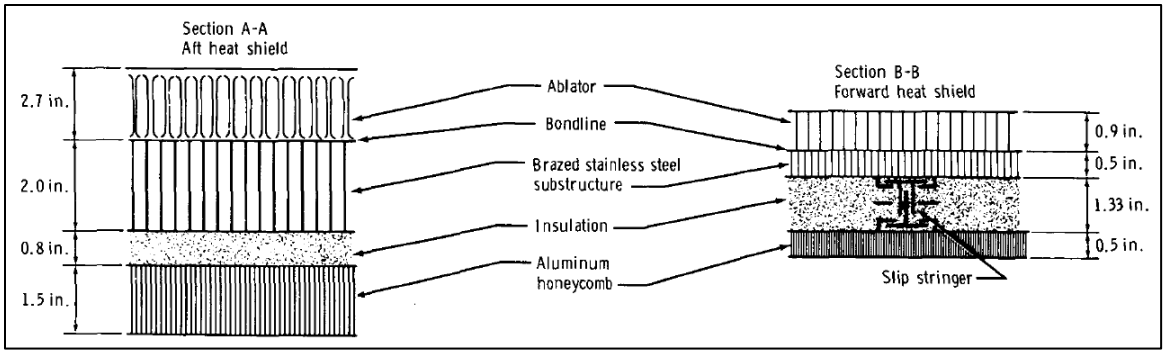

Figure 2. Multi-Layer Apollo TPS. Source: [6].

The process requires to manufacture the TPS was complex. First, brazed sandwich panels of stainless steel were welded together, then the structure was cleaned with an abrasive detergent slurry and coated with a primer; next, the fiberglass honeycomb was secured to the structure with adhesive tape, and the ablative Avcoat material was applied by injecting it into the honeycomb cells (Figure 3) before 32 hours of curing/post-curing and post-processing to include machining and applying a sealant coating [6].

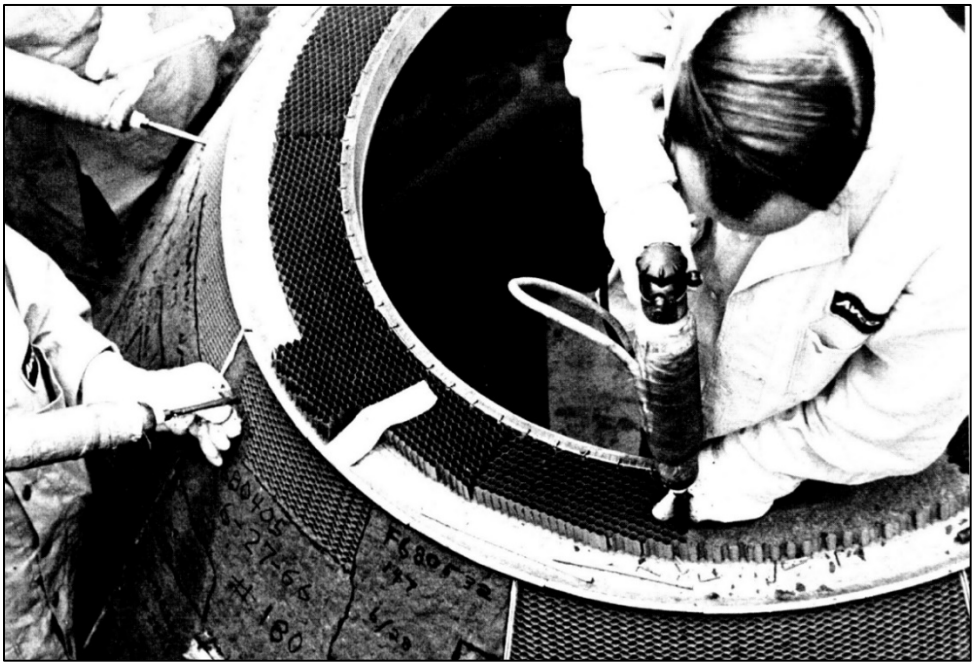

Figure 3. Injection of Avcoat Ablative into Honeycomb Cells. Source: [6].

The National Aeronautics and Space Administration (NASA) used Avcoat for the Orion capsule, first used during the Apollo program; the manufacturing process was complex and required hand assembly with nine total stages (Figure 4) [3].

Figure 4. Nine-Stage Avcoat Display. Source: [3].

NASA also used Phenolic Impregnated Carbon Ablator (PICA), which has a lower density (~270 kg/m^3), for applications including the Stardust mission and the Mars Science Lab (MSL); a variant was also used in SpaceX's Dragon cargo vehicle [3].

NASA's space shuttle program uses a non-ablative TPS consisting of tiles. These insulative and reusable tiles manage thermal energy via storage and re-radiation, leaving the material unchanged; this is done by coating the structural material in low conductivity insulating material and applying a thin coating with high emissivity [3]. Silica-based fibers make up the high porosity (>90% porosity) and low density (140 to 190 kg/m^3) insulating layer, which protects the aluminum sub-structure of the shuttle [3]. Depending on the location on the shuttle an RCG or TUFI coating is applied to provide high surface emittance and impact protection from debris [3].

NASA has continued TPS research by investigating reusable metallic TPS. Metallic TPS designs seek to decouple the thermal and structural functions via a metallic shell to contain internal isolation, maintain shape, and withstand mechanical loads [7]. The current design is a superalloy honeycomb sandwich (Figure 5) [7].

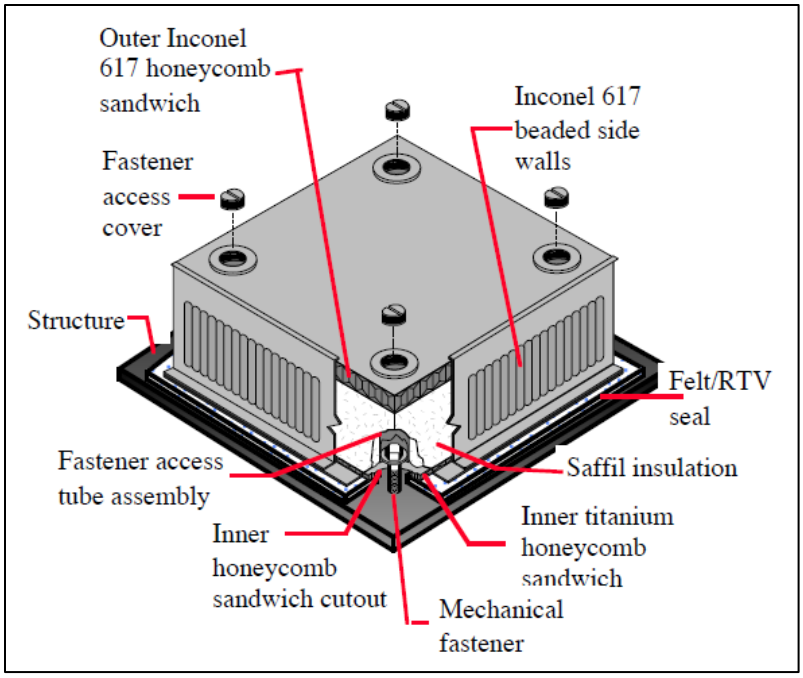

Figure 5. Superalloy Honeycomb Sandwich TPS. Source: [7].

Recent research suggests the use of high-performance ceramics for TPS materials; C-SiC ceramic matrix composite (CMC) structures have been sandwiched with SiC foam for improved efficiency (Figure 6) [7]. The middle layer has a lattice structure to facilitate the passage of a coolant for active temperature control [7].

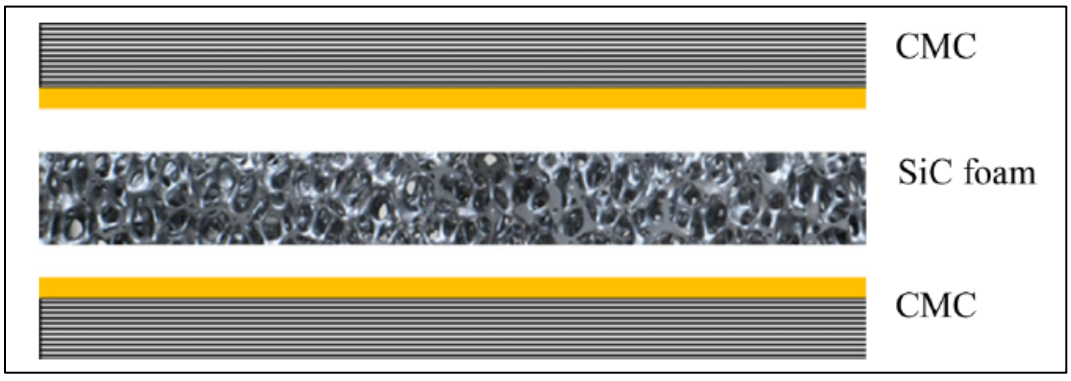

Figure 6. CMC Sandwich TPS Concept. Source: [7].

As TPS research continues, improved concepts are designed. Self-healing TPS materials have been proposed where CMC microcracks seal before oxygen penetrates the inner fibers [8]. Additionally, AM has been explored as a means of manufacturing TPS materials [9].

2. Additive Manufacturing

Additive Manufacturing (AM), commonly called "3D printing," is the manufacturing of components layer by layer. AM offers several advantages to conventional manufacturing, such as greater customization, complex geometries, internal features, material gradients, and more; these advantages allow for improved performance and efficiency [10]. AM technology has been used with many types of materials, to include polymers, ceramics, and metals.

AM has roots reaching back to the 1960s, when an experiment at Battelle Memorial Institute attempted to create solid objects from photopolymers by intersecting two laser beams at different wavelengths [11]. The goal was to polymerize, or solidify, the material at the point of intersection [11]. While this method of manufacturing was never commercialized, it was a precursor to the commercialization of stereolithography in 1987 [11]. Stereolithography is a process that solidifies a photopolymer resin layer by layer using a laser (Figure 7) [11].

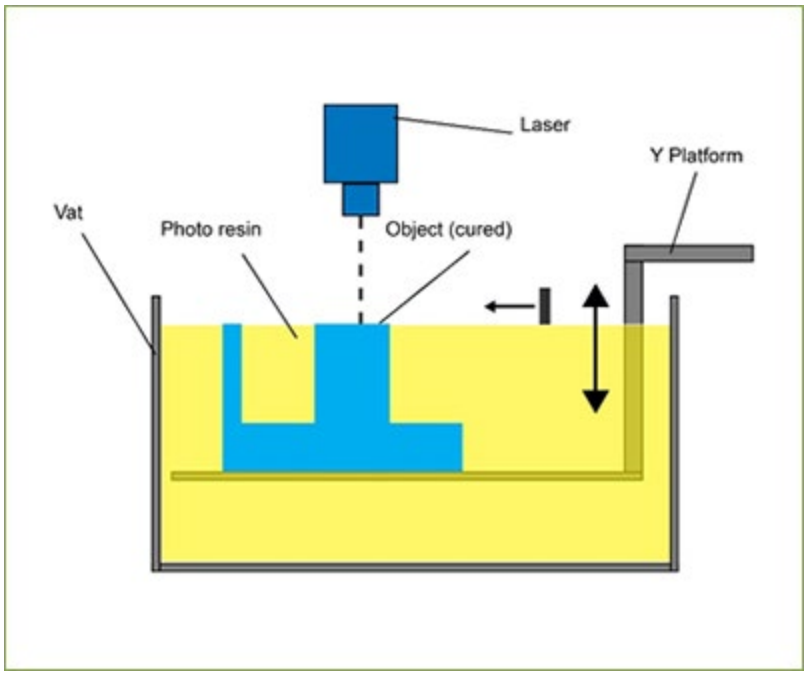

Figure 7. Stereolithography Apparatus (SLA). Source: [12].

Since the development of stereolithography, AM research has continued. The International Organization Standardization and American Society for Testing and Materials (ASTM) classify AM processes into the following seven categories: (1) binder jetting (BJ), (2) directed energy deposition (DED), (3) material extrusion (ME), (4) material jetting (MJ), (5) powder bed fusion (PBF), (6) sheet lamination (SL), and (7) vat polymerization (VP) [10]. A much newer method of ME is Vibration Assisted Printing (VAP), which allows for the printing of highly viscous, clay-like material [13]. This method uses high-amplitude vibrations to induce controlled flow of highly viscous materials under pressure; this method greatly widens the range of feasible materials for AM (Figure 8) [13]. Without the vibration, the material will not flow from the applied pressure alone; however, the flow can be controlled by varying the applied pressure and amplitude of vibration [13].

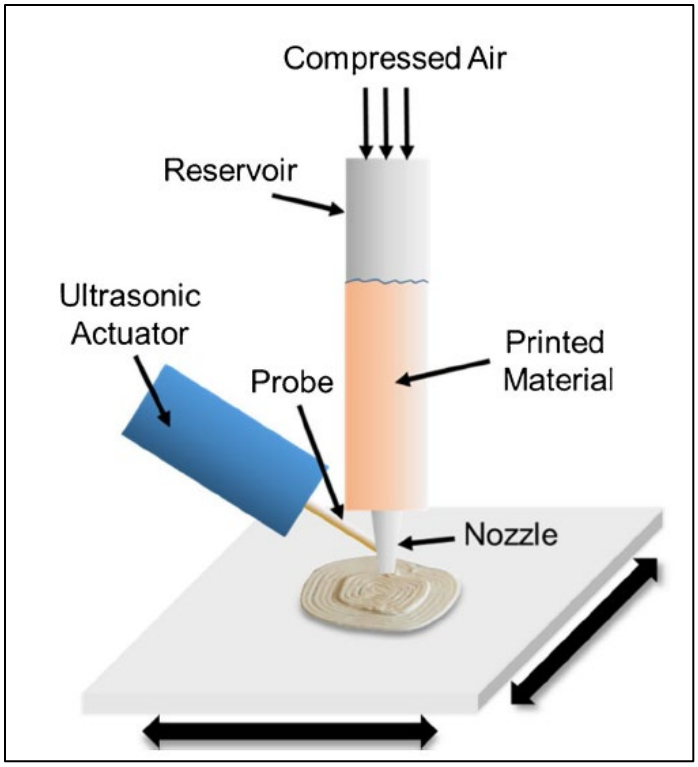

Figure 8. VAP AM Method. Source: [13].

3. Ceramic Matrix Composites

High performance ceramics have been studied and developed for applications such as space transportation systems and advanced friction systems due to their high thermal conductivity, low thermal expansion, and high strength at elevated temperatures [14]. Ceramic composite materials are unique because of their greater strain to failure, nonlinear stress-strain behavior, and low material densities [14]. It is important to note that the properties of CMC depend strongly on the manufacturing method; three methods are currently used for space applications: (1) chemical vapor infiltration (CVI), (2) polymer infiltration and pyrolysis (PIP), and liquid silicon infiltration (LSI) [15]. Pre-ceramic polymers (PCPs) are also used to manufacture CMCs due to cost-reduction, lower processing temperatures, and the ability to create larger and more complex parts [15]. Silicon-based PCPs (Figure 9) are commonly used in manufacturing CMCs [15].

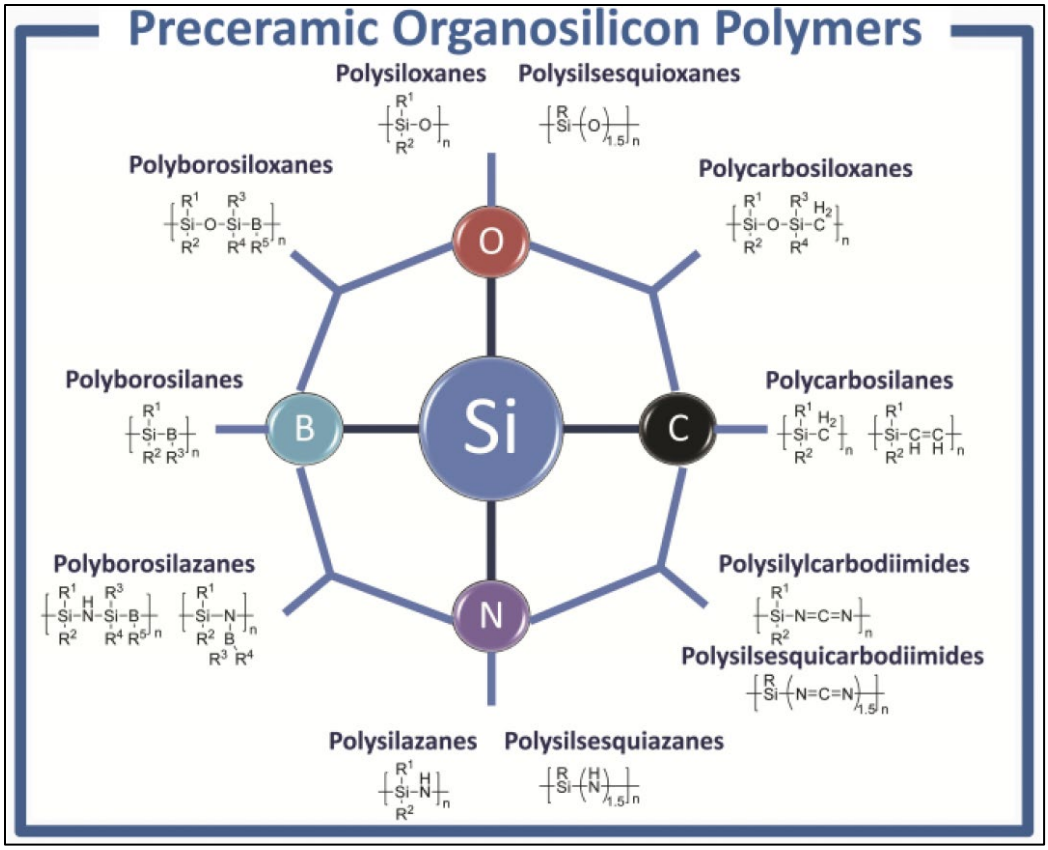

Figure 9. Silicon-Based PCPs. Source: [15].

CMCs are used as brake components for high performance motorbikes and automobiles; these components are made of a preceramic polymer and SiC as a filler with carbon fiber as reinforcement [15]. They are significantly lighter and have a better coefficient of friction with fewer signs of wear when compared to metal components [15]. These components perform with more consistency than the more expensive carbon/carbon rotors. They are lighter and promote overall vehicle performance [15].

SiC can be manufactured into complex shapes at relatively moderate temperatures using a polycarbosilane (PCS) precursor [16]. Ideally, PCS resins have low cure temperatures, high ceramic yield, and excellent thermal stability [16]. The formation of SiC ceramics begins with the shaping of the polymer into the desired object and thermally curing the object. The cured polymer is then crystallized via pyrolysis (Figure 10) [15]. These ceramics are highly porous after pyrolysis due to significant weight loss and volume

shrinkage from the removal of organic groups and elements [17]. Ceramic SiC powders can also be introduced prior to curing to optimize the formation of the ceramic to achieve desirable properties [17].

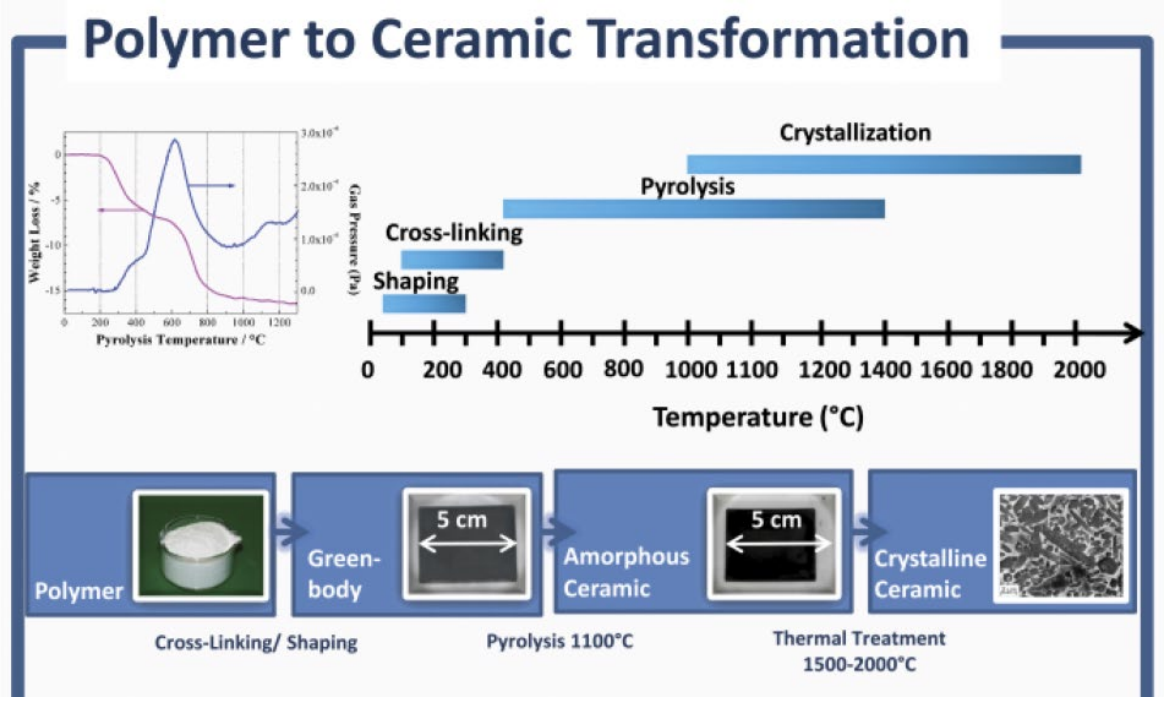

Figure 10. Polymer to Ceramic Transformation. Source: [15].

4. Characterization of Additively Manufactured Products

Additively manufactured components must be characterized to understand the mechanical and thermal properties as well the microstructure. Microstructure analysis can help to understand the properties exhibited by the manufactured components. Characterization of the material can help for optimization of the manufacturing process to ensure desired properties are exhibited. Manufactured components are typically tested using several methods including, but not limited to, mechanical testing, optical microscopy, scanning electron microscopy (SEM), energy-dispersive x-ray spectroscopy (EDS), x-ray powder diffraction (XRD), x-ray computed tomography (CT), and thermal testing. Mechanical testing is used to determine the elastic modulus, yield strength, and ultimate tensile strength. SEM and optical microscopy are used to investigate the microstructure of

a material. CT scanning can be used to generate a 3D model of a component to reveal pores or irregularities non-destructively. EDS and XRD are used to evaluate the composition of a material. Thermal testing can be conducted to estimate the thermal conductivity of a material. These common testing methods can be used to characterize a material and determine if it is suitable for a desired application.

C. OBJECTIVES

The objective of this research is to investigate the effects of pyrolysis temperature and additives, on SiC forming mixtures of preceramic polymers and powders and how they influence the final phase. Preceramic polymers are known to form different forms of SiC upon pyrolysis depending on the temperature. Amorphous SiC starts to form at 800°C, which then nucleates to nanocrystalline β-SiC at 1200°C and completely transforms at 1500°C. However, the phases that form during pyrolysis can be influenced by seed powders to promote nucleation at lower temperatures. Therefore, it is possible to create mixtures of SiC forming polymers and crystalline SiC powders that will have a different phase transformation sequence.

Testing samples will be mixed, cured, and then heated slowly in a furnace to various temperatures and pyrolyzed into a ceramic. Various seeding mechanisms will be used to explore the effects. The relationship between the initial components and the final products will help characterize the effects of the pyrolysis parameters. The effects of heating will be investigated for six different sample configurations: a pure polymer sample, two pure polymer samples with a layer of SiC powder (micro and nano particles), a polymer mixture with 80–85 wt% of SiC powder, a sample with an embedded carbon-loaded PLA layer, and a sample with crystalline graphite. SEM imaging will be employed to characterize the microstructure and composition of each sample. This study will explore the effect that different sample configurations and furnace temperatures have on the final microstructure of ceramic samples.

Understanding how the microstructure is affected by various heat treatments and additives can improve fabrication processes and help predict the performance and viability of materials in such applications. Based on this research, it is possible to characterize the

relationship between pyrolysis parameters and the properties of the final product. This information can be then used to further optimize the manufacturing process of high-performance ceramics to achieve the desired properties for various applications such as AM of ceramics.

THIS PAGE INTENTIONALLY LEFT BLANK

II. EXPERIMENTAL METHODS

A. MATERIALS

The preceramic liquid polymer used in this study is StarPCS SiC Matrix Precursor 10 (SMP-10), from Starfire Systems. This material is a polycarbosilane and forms SiC during pyrolysis. SMP-10 is the only SiC precursor that is a liquid at room temperature and has a near-stoichiometric yield for silicon and carbon [18]. Amorphous SiC has been reported to form at 850–1200°C and crystalline SiC at 1250–1700°C [18]. The aged batch was stored at room temperature and slowly, partially cured over the course of a year; however, the new batch was stored in a refrigerator as recommended by the manufacturer (Figure 11).

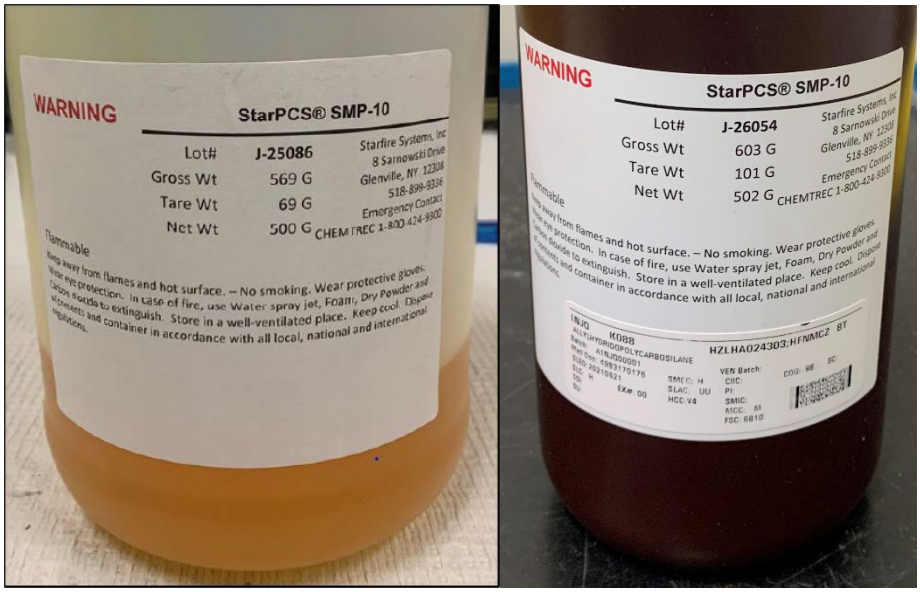

Figure 11. SMP-10 SiC Precursor Polymer (Aged on Left, New on Right)

Various nucleation aids will be added to or mixed with SMP-10. These nucleation aids include micron crystalline SiC powder, nano-powder SiC, crystalline graphite mixed with UV-curable polymer (AM filament), amorphous carbon-loaded PLA layer (printed via AM). The six sample types are summarized in Table 1.

Table 1. Initial Sample Configurations

Pure	SMP-10
Micron	Micron Crystalline SiC Powder with SMP-10
Nano	Nano SiC Powder with SMP-10
PLA	3D Printed Amorphous Carbon-Loaded PLA Layer with SMP-10
Graphite	Crystalline Graphite Mixed with UV Polymer (65 wt%) with SMP-10
Mixed	SiC Powder and SMP-10 Mixture (85 wt%)

B. SAMPLE PREPARATION

1. Sample Mixing

The mixed samples required using a high-speed mixer (Figure 12) to combine the liquid polymer and the SiC powder. The SMP-10 and the SiC powder were combined in mixing cups (Figure 13) and stirred with a spatula before being placed in the speed mixer.

Figure 12. FlackTek SpeedMixer

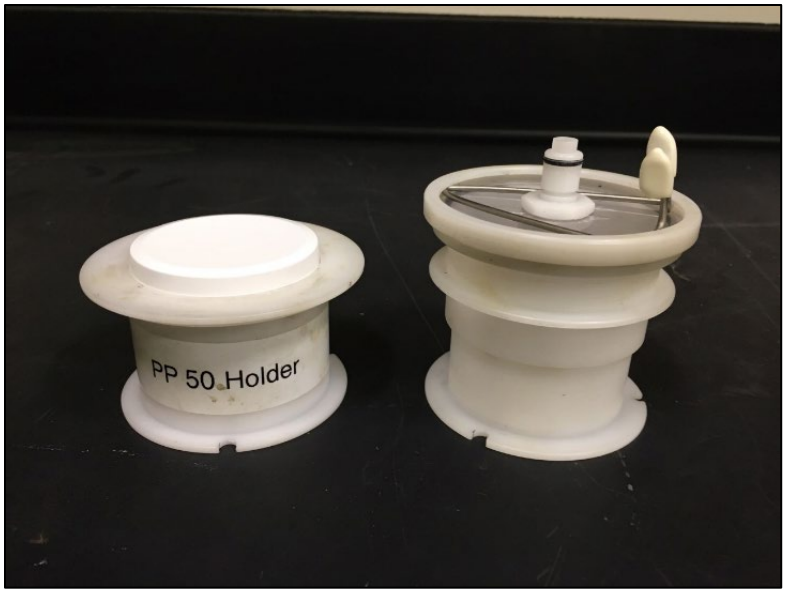

Figure 13. Mixer Cups

Creating this mixture allows the material to be molded into a desired shape before it is cured and hardened and then pyrolyzed into a ceramic. This mixture can also be used with AM via VAP to fabricate more complex geometries.

2. Sample Molding

For this research, all sample types were initially placed or molded into a silicone tray (Figure 14) to form cubic samples. At first, the nucleation aids were placed in the tray and the remainder of the tray volume was filled with SMP-10. No mixing was required. The micron and nano SiC powders were carefully added to each cell as to form a complete bottom layer. The carbon-loaded PLA layers were placed in the bottom of each cell so that the build plate side of the layer was oriented downwards before filling with SMP-10. The graphite filament extrudate was simply placed at the bottom of each cell. After all the nucleation aids were all added to the respective cells of the silicone tray, pure SMP-10 was added to fill the remaining volume in each cell.

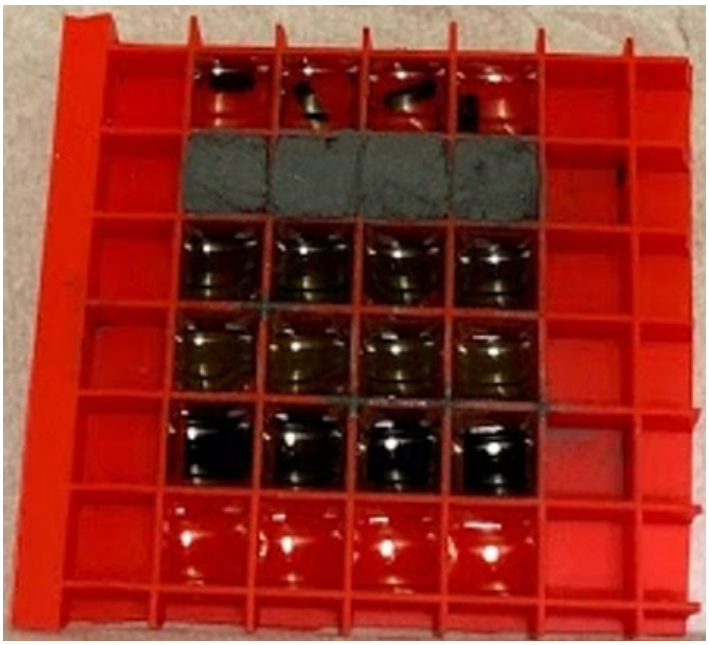

Figure 14. Pre-Cured Samples

3. Sample Curing

Initial curing stages (Type 1–4,6) (Table 2) were conducted in the vacuum oven (Figure 15) and the final curing stage (Type 5,7-8) was conducted in the tube furnace. Initially, the SMP-10 was used as-is out of refrigerated storage to create each sample type.

Table 2. Curing Procedures

	Step 1	**Step 2**	**Step 3**	**Step 4**	**Step 5**
Type 1	70°C, air, 4hr	100°C, air, 4hr	248.8°C, vac, 4hr		
Type 2	70°C, air, 4hr	100°C, air, 4hr	130°C, air, 4hr	248.8°C, vac, 4hr	
Type 3	70°C, air, 4hr	100°C, air, 4hr	130°C, air, 4hr	130°C, air, 12hr	248.8°C, vac, 4hr
Type 4	130°C, Argon, 8hr				
Type 5	300°C, 2°C/min, 4hr	350°C, 2°C/ min, 4hr	400°C, 2°C/min, 4hr	20°C, 2°C/min	
Type 6	140°C, Argon, 8hr				
Type 7	250°C, 2°C/min, 4hr	300°C, 2°C/ min, 4hr	350°C, 2°C/min, 4hr	400°C, 2°C/min, 4hr	20°C, 2°C/ min
Type 8	250°C, 2°C/min, 1hr	300°C, 2°C/ min, 1hr	350°C, 2°C/min, 1hr	400°C, 2°C/min, 1hr	20°C, 2°C/ min

Figure 15. Thermal Vacuum Oven (TVAC)

The first batch of samples were cured using Type 1 listed in Table 1. However, the SMP-10 was not fully hardened and began to bubble when the vacuum was pulled before Step 3 started. Therefore, the polymer pre-processing treatments were conducted to ensure future samples were fully cured. Then cure Type 2 was used starting with Step 3 to completely hardened the samples. However, during Step 4, the vacuum oven shut off due to over temperature protection settings.

Polymer pre-treatment (Table 3) was introduced to remove the most volatile species in the liquid polymer to minimize mass loss and bubbling or shrinkage later during the curing and sintering processes [19]. The polymer behaved in an unexpected way compared to the previous batch from the same manufacturer and a pre-curing procedure was developed to minimize escaping gas at elevated temperatures (as low as 130°C), and ensure samples fully cured.

Table 3. Polymer Pre-Processing Treatments

	Step 1	**Step 2**	**Step 3**
Type 1	80°C, air, 10hr		
Type 2	130°C, vac, 1hr	130°C, air, 12hr	
Type 3	130°C, vac, 1hr	100°C, air, 12hr	
Type 4	80°C, vac, 36hr	100°C, air, 4hr	130°C, air, 4hr

The second batch of samples were prepared with SMP-10 that was pre-treated (Type 1) and then cured (Type 2); however, they began to bubble during Step 3. Some of the samples were removed from the silicone mold before they were completely hardened. The remainder of the samples were left in the tray as curing resumed (Type 3 Step 4). Before the final stage (Type 3 Step 5), the rest of the samples were removed from the mold; it was observed that they had all crumbled during the curing process due to bubbling earlier. The mixed samples never experienced any bubbling or crumbling of any kind. Again, the vacuum oven shut off during the 248.8°C cycle due to over temperature protection. The dial was adjusted to avoid further failed runs.

Further polymer pre-treatments were tested by varying temperature, cycle duration, etc. Bubbling occurs at 130°C (Type 2), but the polymer was not fully hardened at 100°C (Type 3). Increasing the surface area of SMP-10 exposed allowed more gas to escape before creating the samples and starting the curing process.

The new batch of SMP-10 was not cured in the same way as the old batch, and there was a notable interaction between the liquid polymer and the silicone tray at elevated temperatures forming hydrogen gas. With little progress using the new batch of SMP-10, the old batch of SMP-10 was used in conjunction with a solvent to make the material usable again with nucleation aids. Therefore, allowing the effect of nucleation aids to be investigated despite the unexpected behavior of the new batch of SMP-10.

For the third batch of samples, the aged SMP-10 was used; it had a jelly-like consistency. Small pieces were cut to relative size and a solvent was applied as the nucleation aids were paired with the SMP-10. Each sample type was placed in a container that would not melt or have a similar interaction with the material as the silicone tray during cuing (Type 4) and sealed with Argon gas in the container. Following this curing stage, the samples were moved to alumina boats to be placed in the tube furnace (Figure 16) for further curing (Type 5).

Figure 16. Lindberg Blue M Furnace Chamber and Control Console

A fourth batch of samples created using a new sample preparation procedure. Seed powders (nano, fine micron, coarse micron) and the new SMP-10 were placed in containers sealed with Argon and initially cured (Type 6) in the vacuum oven. The final curing (Type 7) and pyrolysis (Type 2) were done together in one step before cooling.

The samples from batch four were mounted in a such a way that was difficult to see the seed powders and their effect under the SEM. Therefore, a fifth batch of samples was made with the new SMP-10 and a modified curing (Type 8) and sinter procedure (Type 5) due to the small size. The dwell times at each target temperature were reduced to one hour.

4. Sample Pyrolysis

All pyrolysis was conducted in the tube furnace. Again, samples were placed in alumina boats and moved to the center of the tube. Fire bricks were used as insulation inside and outside the tube on both sides of the furnace. This insulation can prevent the formation of a temperature gradient in the tube outside the furnace; this thermal gradient in conjunction with rapid heating and cool gas flow can lead to cracking of the alumina tubes. Gaskets were attached to achieve a proper seal to prevent any of the argon gas that was pumped through the tube during the heating cycle from escaping. Various programs were written for each desired heating cycle (Table 4).

Table 4. Sintering Procedures

	Step 1: Ramp Up	**Step 2: Dwell**	**Step 3: Ramp Down**
Type 1	800°C at 2°C/min	4 hours	20°C at 2°C/min
Type 2	1000°C at 2°C/min	4 hours	20°C at 2°C/min
Type 3	1200°C at 2°C/min	4 hours	20°C at 2°C/min
Type 4	1400°C at 2°C/min	4 hours	20°C at 2°C/min
Type 5	1000°C at 2°C/min	1 hour	20°C at 2°C/min

A summary of each batch of samples is given in Table 5. Batch 1 and Batch 2 were not usable after bubbling and crumbling.

Table 5. Sample Batches

Samples	**Pre-Treatment**	**Curing**	**Sinter**
Batch 1	None	Type 1 and 2	None
Batch 2	Type 1	Type 2 and 3	None
Batch 3	None	Type 4 and 5	Type 1–2
Batch 4	None	Type 6 and 7	Type 2
Batch 5	None	Type 8	Type 5

C. SAMPLE CHARACTERIZATION

Following sample preparation, the material can be examined with either the SEM (Figure 17) or optical microscope. The SEM fires electrons through a series of magnetic lenses that hit a sample; the detection of the deflected electrons forms an image. Images formed using an SEM can achieve more than 300,000x magnification, which is significantly greater than the nominal ~1,000x magnification achieved by light microscopes [20]. Optical microscopes offer significantly less magnification, but does form images with color contrast unlike the SEM. Both forms of microscopy serve as methods to visually observe samples to better understand the microstructure of materials. Uniformity of structure, porosity, and grain structure are all aspects that can be observed.

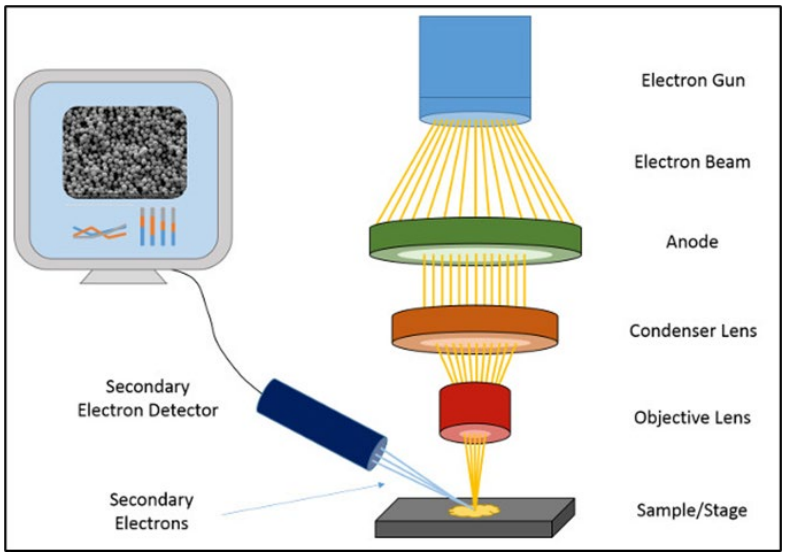

Figure 17. SEM Schematic. Source: [20].

THIS PAGE INTENTIONALLY LEFT BLANK

III. RESULTS AND DISCUSSION

A. PYROLYSIS

Batch 3 samples that underwent successful pyrolysis at 800°C are seen in Figure 18. Cracking and breaking apart were observed and it was difficult to distinguish between the samples. To prevent further mixing during pyrolysis, different compartments were constructed in a separate ceramic boat using alumina pieces (Batch 4). These provided some separation, but some mixing was still observed as the alumina pieces shifted during removal of the boat from the furnace. For the next batch (Batch 5), these pieces were adhered to the alumina boat using a yttria-based ceramic paste, which prevented these issues.

Figure 18. 800°C Pyrolysis (Batch 3)

Batch 3 samples for 1000°C experienced oxidation during pyrolysis due to insufficient argon gas flow or a leak in the seal of the tube furnace. Batch 4 (Figures 19–20) samples were also unusable due to the mounting orientation of the samples on the SEM stubs after pyrolysis and potential mixing between the sample types. Batch 5 (Figures 21–22) samples were successfully pyrolyzed at 1000°C with three different seed powders and properly mounted for viewing under the SEM.

Figure 19. Batch 4 before 1000°C Pyrolysis

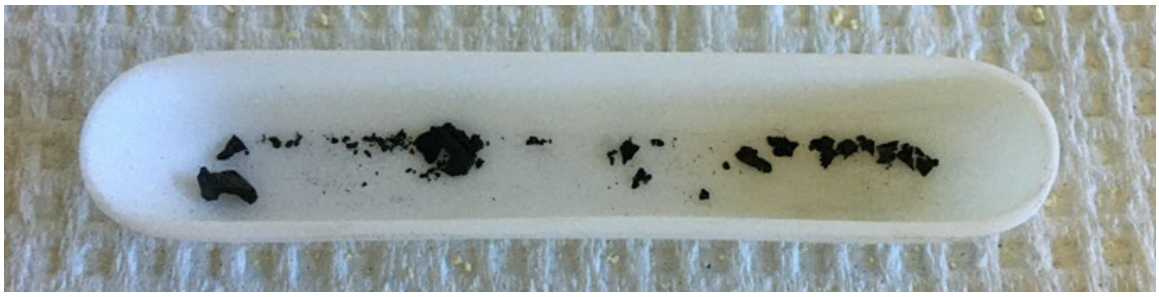

Figure 20. Batch 4 after 1000°C Pyrolysis

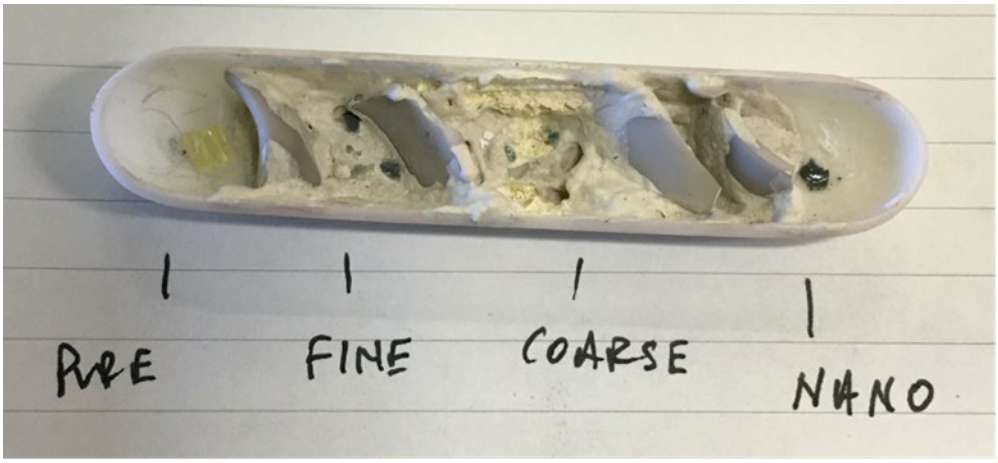

Figure 21. Batch 5 before 1000°C Pyrolysis

Figure 22. Batch 5 after 1000°C Pyrolysis

B. SCANNING ELECTION MICROSCOPE (SEM) IMAGING

1. Batch 3

Significantly less cracking is observed in the Batch 3 samples (Figures 23–25) compared to later batches. It was observed that the samples appeared white-grey in color, which typically originates from oxide formation on the surface, suggesting that there was a leak in the tube furnace seal or insufficient argon gas flow. The Pure SMP-10 (Figure 23) surface appears to be smooth without noticeable clusters of SiC grains that might have formed during pyrolysis.

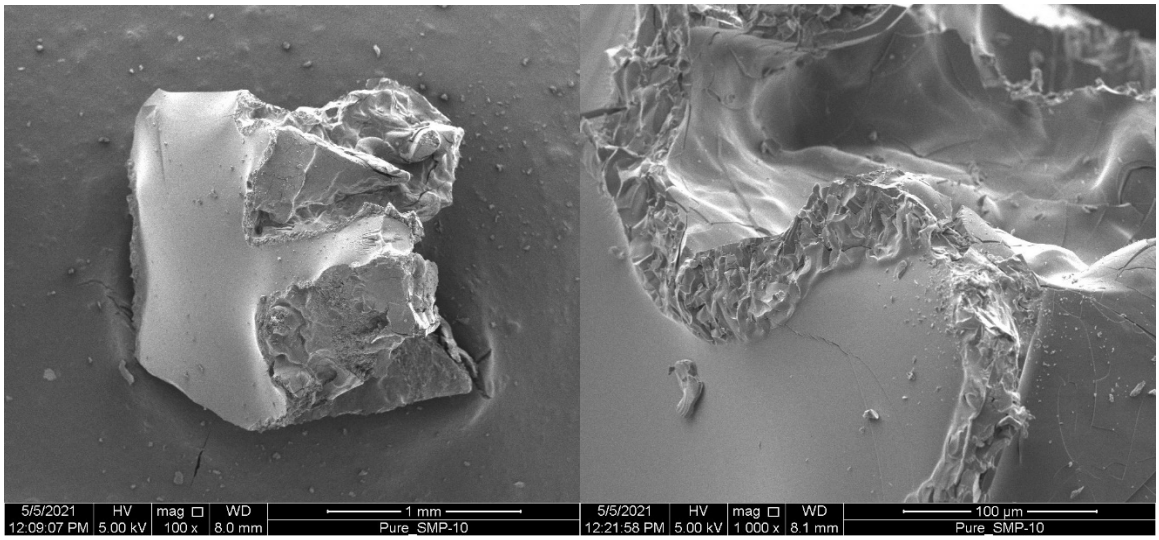

Figure 23. Pure Sample after 1000°C Pyrolysis (Batch 3)

The micron and nanometer particles can be observed on the surface of each respective sample. The micron powders appear to be more jagged and rough, while the nano particles appear more spherical. The powders were fused together with featureless regions that form during pyrolysis of the pre-ceramic polymer. It was interesting to note that there was no discernable boundary between the powders and the polymer sections.

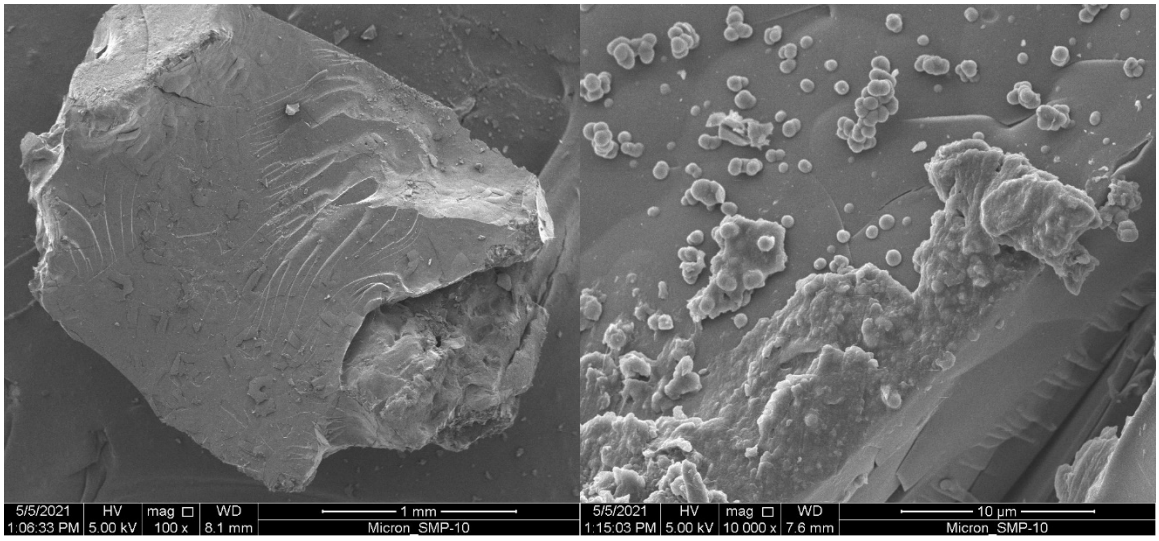

Figure 24. Nano Sample after 1000°C Pyrolysis (Batch 3)

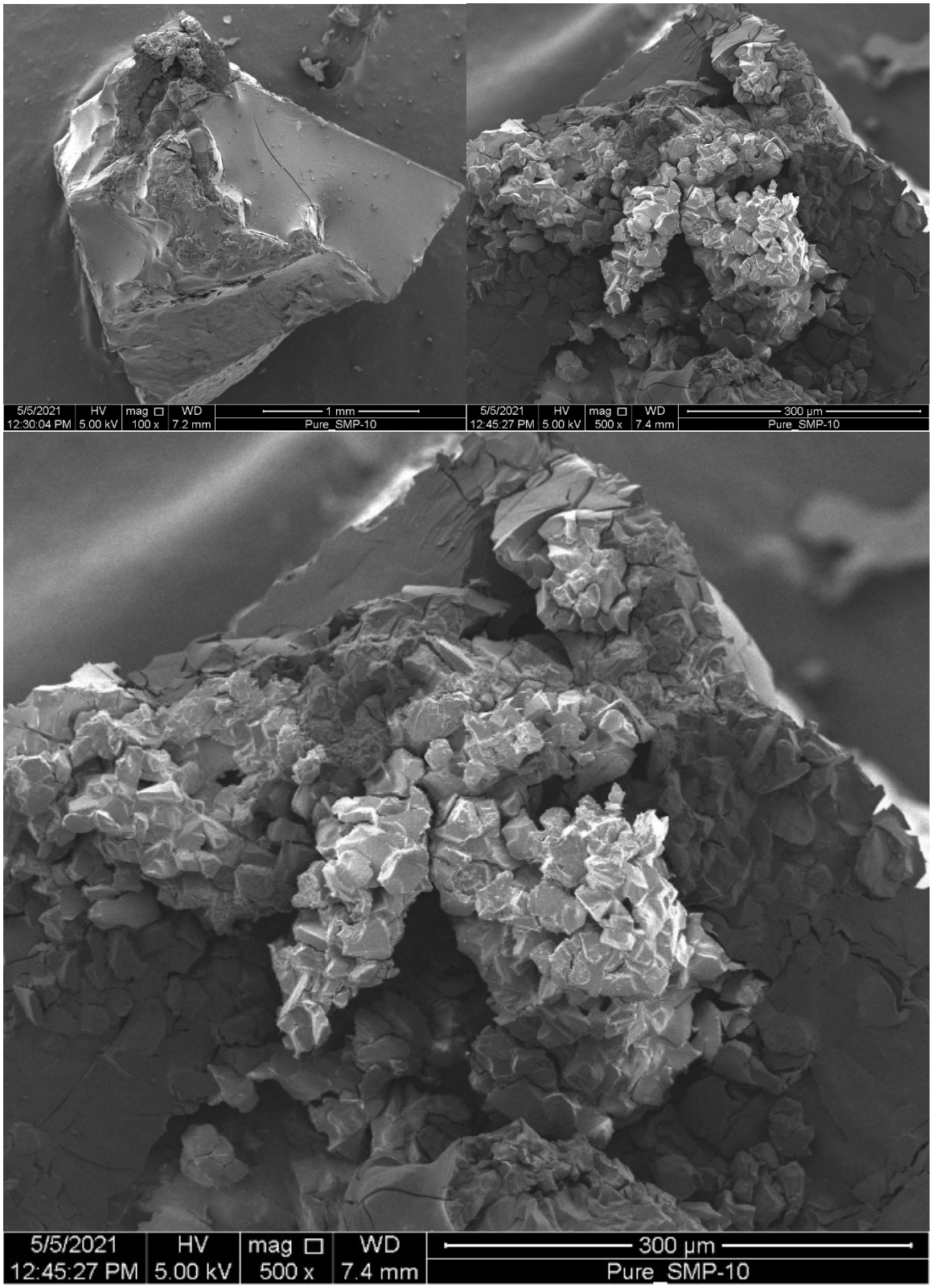

Figure 25. Micron Sample after 1000°C Pyrolysis (Batch 3) with the Same Image in a Larger Size

2. Batch 4

Batch 4 samples (Figures 26–30) underwent successful pyrolysis at 1000°C. The samples appear to be black and glassy visually, suggesting oxidation was not a factor as it was for Batch 3 samples. Again, the Pure SMP-10 sample has mostly smooth surfaces with no noticeable fine particles or grain formation.

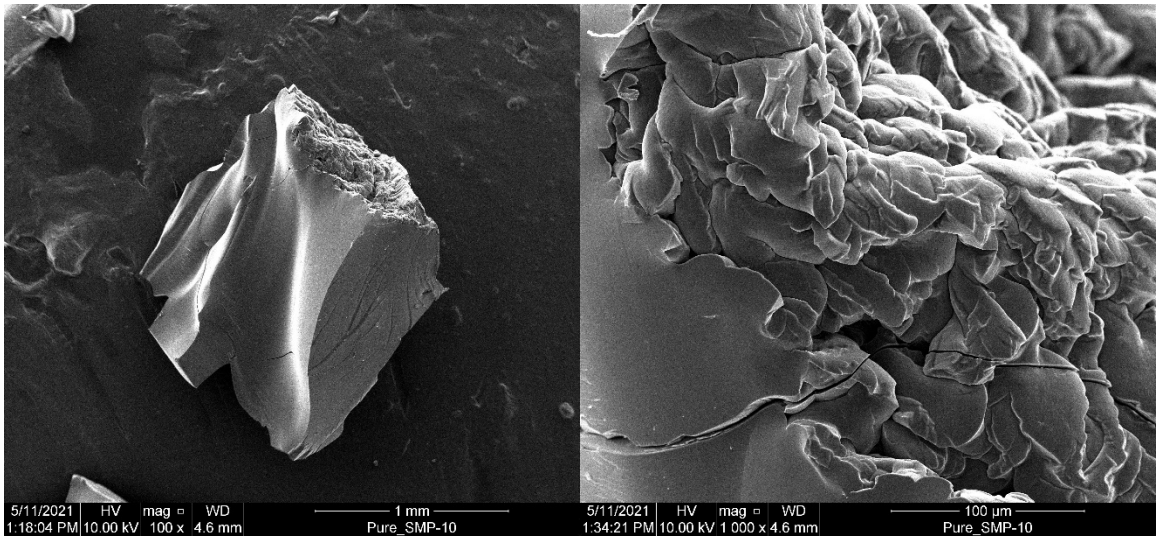

Figure 26. Pure Sample after 1000°C Pyrolysis (Batch 4)

For each seed powder used, a sample was investigated before and after pyrolysis. The surface of the fine micron powder sample before pyrolysis was relatively smooth with fewer particles than expected. The post-pyrolysis fine micron powder sample exhibited noticeable cracks with a much rougher surface and larger groupings of particles. These cracks form in all samples as the polymer shrinks due to pyrolysis.

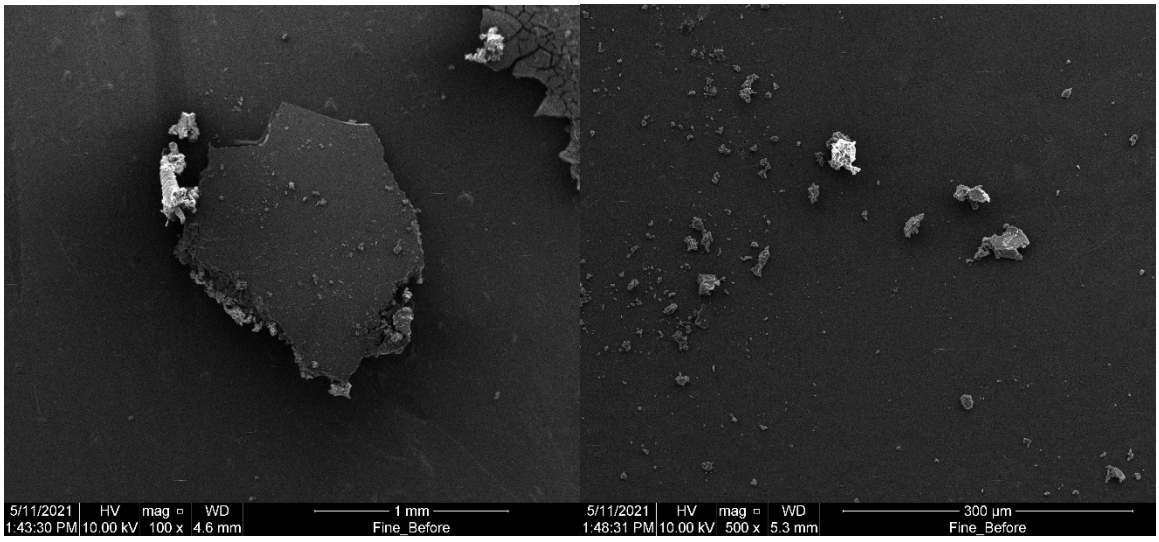

Figure 27. Fine Micron Sample before 1000°C Pyrolysis (Batch 4)

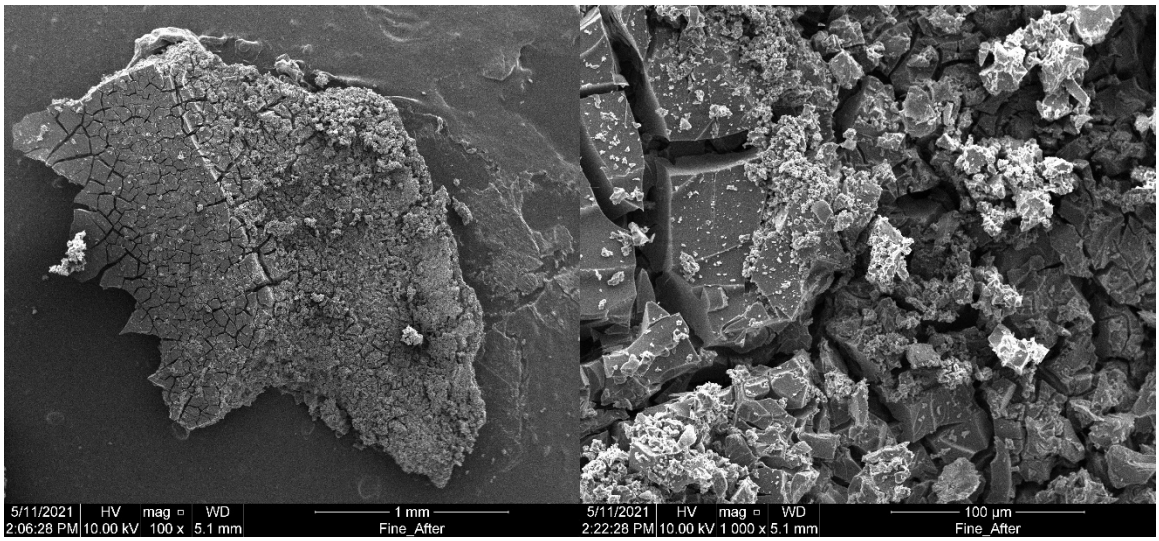

Figure 28. Fine Micron Sample after 1000°C Pyrolysis (Batch 4)

The nano powder sample pre-pyrolysis also had relatively smooth surfaces. While the post-pyrolysis sample exhibited more cracking, it was also relatively smooth overall. This was potentially due to an inappropriate mounting orientation, in which the particles themselves were mostly out of view of the SEM.

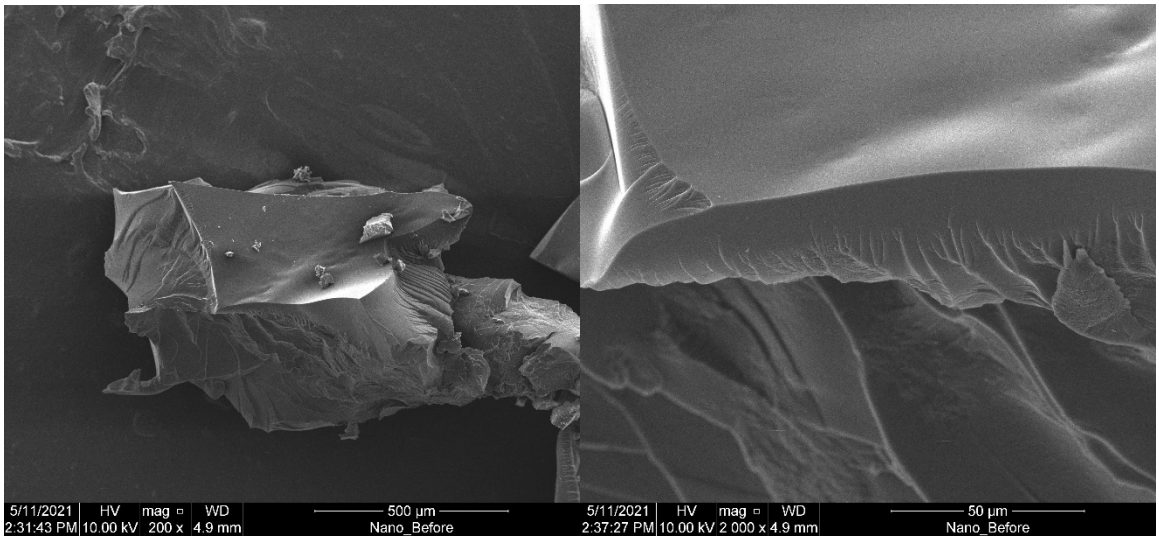

Figure 29. Nano Sample before 1000˚C Pyrolysis (Batch 4)

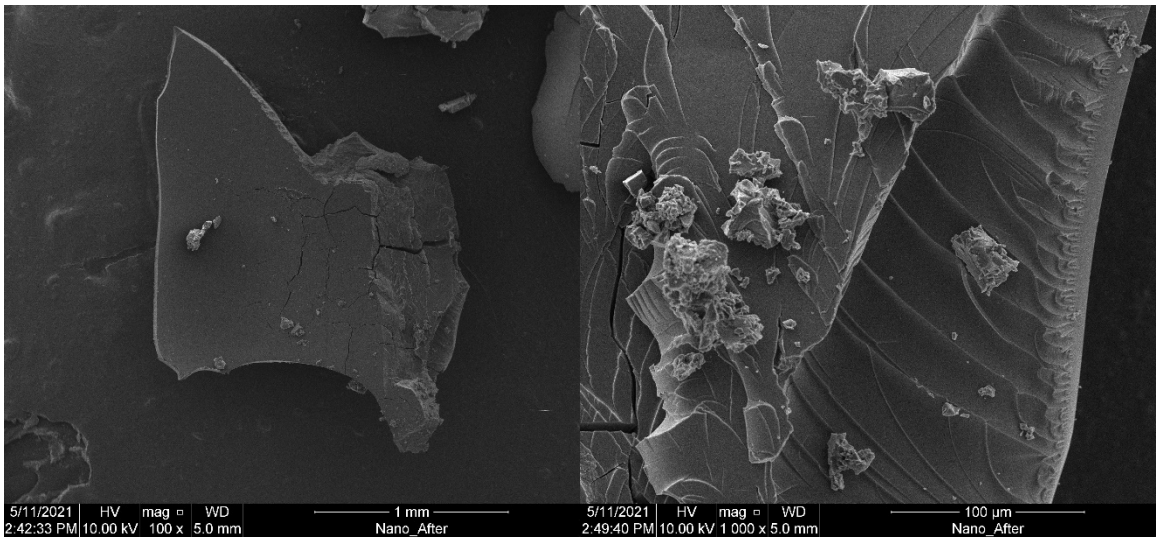

Figure 30. Nano Sample after 1000˚C Pyrolysis

3. Batch 5

Only the post-pyrolysis samples were investigated for Batch 5 (Figures 31–33). Samples were viewed under the optical microscope to determine the appropriate mounting orientation for viewing under the SEM to be able to focus on particle-polymer interfaces for all samples. Additionally, two samples for each seed powder type were viewed to better understand the characteristic features for each seed powder.

As before cracking was observed as well as particle agglomerates due to polymer pyrolysis that causes shrinkage. The fine micron powder sample appears to form carbon black; however, it is most likely from the graphite paint and not SMP-10. The nano powder sample had surface irregularities that could potentially be a result of the seed powder.

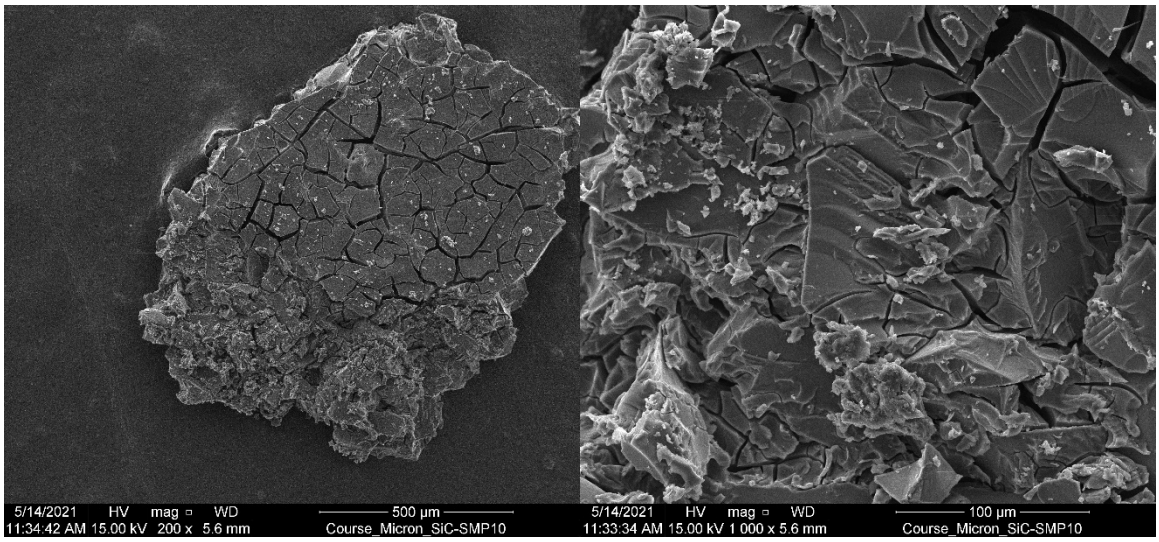

Figure 31. Coarse Micron Sample after 1000°C Pyrolysis (Batch 5)

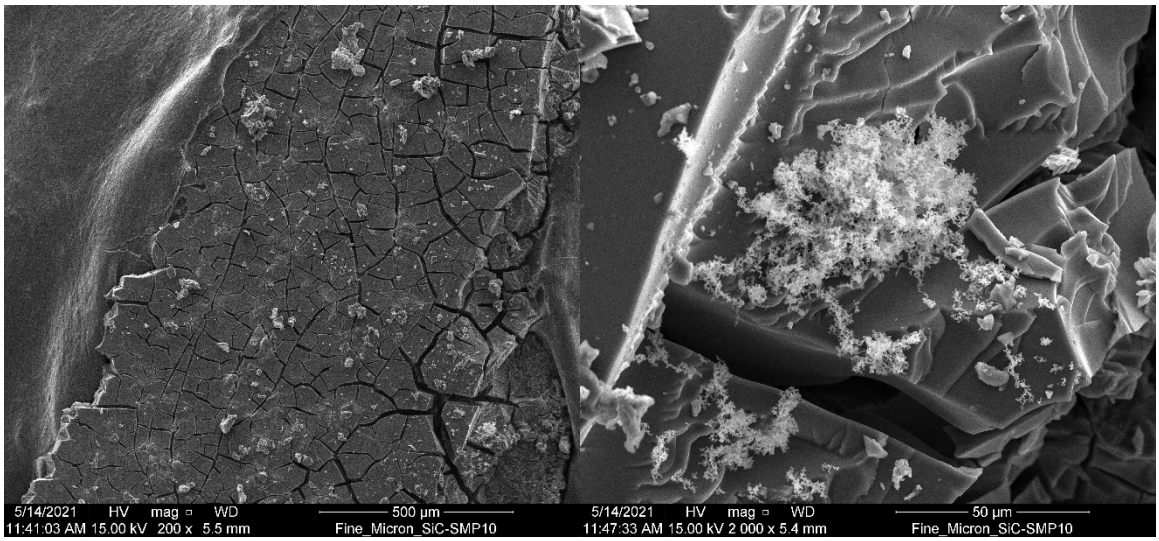

Figure 32. Fine Micron Sample after 1000°C Pyrolysis (Batch 5)

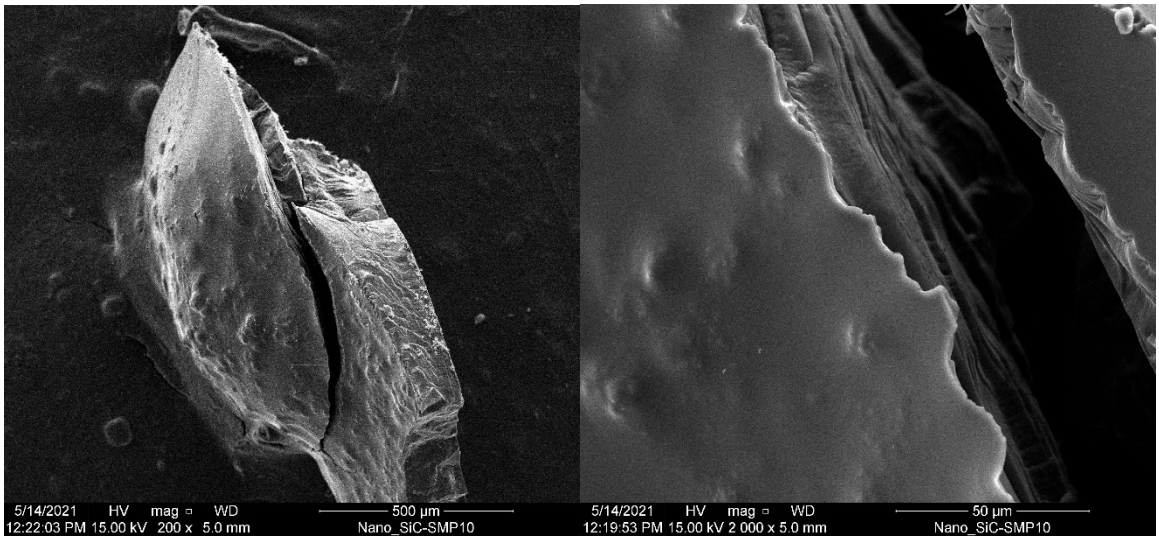

Figure 33. Nano Sample after 1000°C Pyrolysis (Batch 5)

Overall, it was hard to distinguish the boundaries between the seed particles and the pyrolyzed polymer. All the powders used had similar morphologies as the pyrolyzed polymer, with smooth surfaces and brittle fracture zones that are characteristic of SiC. The limited number of agglomerates of particle-polymer sections had no visible phase boundaries between the crystalline powders and the pyrolyzed polymer. It is possible that the polymer in these regions might have grown epitaxially from the seed powders as postulated. However, SEM is insufficient to resolve these features and TEM is necessary to be able to look at the crystallinity at these sections.

IV. CONCLUSIONS

The new batch of the pre-ceramic polymer SMP-10 posed challenges during initial curing trials. Bubbling occurred around 130°C, but the polymer was not fully hardened at 100°C. This behavior was observed while molding samples in a silicone tray, which was due to chemical interactions between the polymer and the silicone, possibly generating hydrogen gas. Various pre-curing polymer treatments were investigated to partially cure the SMP-10 before molding the samples. Different containers were used to eliminate this behavior. The exposed surface area of the polymer was initially increased to allow a greater amount of volatiles to escape. The aged and gelled batch of SMP-10 was used with a solvent to create samples that consist of the gel doped with nano-microscale SiC powders. The powder to polymer ratio was increased to eliminate bubbling with the new batch of SMP-10 in larger containers for each sample type. For the final batches, the new SMP-10 was used by first curing it at 140°C in closed containers filled with argon gas, which increased the yield and prevented polymer oxidation, while enabling hardening of the polymer. The mixtures were then pyrolyzed under Argon flow at 800°C and 1000°C to convert the polymer to SiC.

From the images taken with the SEM, the effect of the various seed powders was difficult to observe due to the similarities in the morphology of the crystalline powders and the pyrolyzed polymer that might be amorphous or crystalline. There were no phase boundaries that could be clearly identified in SEM. Further characterization methods such as TEM may be required to determine the degree of crystallization and sample morphology at the interfaces. The seed powders' effectiveness as nucleation aids for epitaxial growth could not be determined with absolute certainty from this research alone, although some SEM images suggest this might have happened at certain locations. Higher resolution TEM imaging can be used to investigate whether the interfaces are amorphous or crystalline in nature and provide a definite answer to these questions.

THIS PAGE INTENTIONALLY LEFT BLANK

V. FUTURE WORK

Further investigation of the interaction between SMP-10 and the silicone tray as well as the plastic containers during curing should be conducted. It would be beneficial to understand the cause of the bubbling that occurs around 130°C. Furthermore, disparity in behavior between the two batches of SMP-10 should be investigated. The possibility of partial curing of the old material may be a factor. Further trials should be run with various temperatures to determine an effect on pyrolysis. Based on the observed effects of nucleation aids in SMP-10, further research could be conducted in which other potential nucleation aids are used.

Additionally, further research in the feasibility of AM with these and similar materials is required. Casting and machine printing can both be used to determine the effects that printing may have on the material properties. Various testing methods could be conducted to determine the mechanical properties of these materials.

THIS PAGE INTENTIONALLY LEFT BLANK

LIST OF REFERENCES

[1] "Space Policy Directives (SPDs)," accessed 08 Apr. 2021. https://www.spacefoundation.org/space_brief/space-policy-directives/.

[2] Wang, Y., Chen, Z., and Yu, S., 2016, "Ablation Behavior and Mechanism Analysis of C/SiC Composites," Journal of Materials Research and Technology, **5**(2), pp. 170–182.

[3] "Thermal Protection Materials and Systems: Past, Present, and Future," accessed 09 Apr. 2021. https://ntrs.nasa.gov/api/citations/20130014035/downloads/20130014035.pdf.

[4] "Returning from Space: Re-entry," accessed 09 Apr. 2021. https://www.faa.gov/about/office_org/headquarters_offices/avs/offices/aam/cami/library/online_libraries/aerospace_medicine/tutorial/media/iii.4.1.7_returning_from_space.pdf.

[5] "A Brief History of Space Exploration | The Aerospace Corporation," accessed 09 Apr. 2021. https://aerospace.org/article/brief-history-space-exploration.

[6] "Apollo Experience Report - Thermal Protection Subsystem," accessed 09 Apr. 2021. https://core.ac.uk/download/pdf/42898643.pdf.

[7] "Reusable Metallic Thermal Protection Systems Development," accessed 09 Apr. 2021. https://ntrs.nasa.gov/api/citations/20040095922/downloads/20040095922.pdf.

[8] Keller, K., Pfeiffer, E., Gaudenzi, P., Lampani, L., Ullmann, T., and Ritter, H., 2005, "Smart Thermal Protection Systems," SAE Transactions, 114, pp. 305–312.

[9] Sulkis, M. C., Driver, J., Saade-Castillo, A., Thompson, A., Wu, H., and Koo, J. H., 2018, "Additive Manufacturing of Thermal Protection System Materials," *2018 AIAA/ASCE/AHS/ASC Structures, Structural Dynamics, and Materials Conference*, American Institute of Aeronautics and Astronautics.

[10] Tofail, S. A. M., Koumoulos, E. P., Bandyopadhyay, A., Bose, S., O'Donoghue, L., and Charitidis, C., 2018, "Additive Manufacturing: Scientific and Technological Challenges, Market Uptake and Opportunities," Materials Today, **21**(1), pp. 22–37.

[11] "History of Additive Manufacturing," accessed 09 Apr. 2021. http://www.wohlersassociates.com/history2016.pdf.

[12] "The 7 Categories of Additive Manufacturing | Additive Manufacturing Research Group | Loughborough University," accessed 09 Apr. 2021. https://www.lboro.ac.uk/research/amrg/about/the7categoriesofadditivemanufacturing/.

[13] Gunduz, I. E., McClain, M. S., Cattani, P., Chiu, G. T.-C., Rhoads, J. F., and Son, S. F., 2018, "3D Printing of Extremely Viscous Materials Using Ultrasonic Vibrations," Additive Manufacturing, **22**, pp. 98–103.

[14] Krenkel, W., 2004, "Carbon Fiber Reinforced CMC for High-Performance Structures," International Journal of Applied Ceramic Technology, **1**(2), pp. 188–200.

[15] Colombo, P., Mera, G., Riedel, R., and Sorarù, G. D., 2010, "Polymer-Derived Ceramics: 40 Years of Research and Innovation in Advanced Ceramics," Journal of the American Ceramic Society, **93**(7), pp. 1805–1837.

[16] Qian, X., Zhou, Q., and Ni, L., 2015, "Preceramic Polymer as Precursor for Near-Stoichiometric Silicon Carbon with High Ceramic Yield," Journal of Applied Polymer Science, **132**(4).

[17] Berbon, M., and Calabrese, M., 2002, "Effect of 1600°C Heat Treatment on C/SiC Composites Fabricated by Polymer Infiltration and Pyrolysis with Allylhydridopolycarbosilane," Journal of the American Ceramic Society, **85**(7), pp. 1891–1893.

[18] "StarPCS SMP-10: Silicon Carbide Matrix Precursor," accessed 09 Apr. 2021. https://www.starfiresystems.com/wp-content/uploads/2018/03/SMP-10.pdf.

[19] Potticary, S. A., 2017, "Chemical and Behavioral Study of Commercial Polycarbosilanes for the Processing of SiC Fibers."

[20] "Scanning Electron Microscopy (SEM) | Protocol," accessed 09 Apr. 2021. https://www.jove.com/v/5656/scanning-electron-microscopy-sem.

INITIAL DISTRIBUTION LIST

1. Defense Technical Information Center
   Ft. Belvoir, Virginia

2. Dudley Knox Library
   Naval Postgraduate School
   Monterey, California